Flavin Recognition by an RNA Aptamer Targeted toward FAD †

ARTICLE *in* BIOCHEMISTRY · MARCH 2002

Impact Factor: 3.02 · DOI: 10.1021/bi015719d · Source: PubMed

4 AUTHORS, INCLUDING:

Manami Roychowdhury Saha
Sequenom, Inc.
5 PUBLICATIONS **198** CITATIONS
SEE PROFILE

Donald H Burke
University of Missouri
63 PUBLICATIONS **1,552** CITATIONS
SEE PROFILE

Flavin Recognition by an RNA Aptamer Targeted toward FAD†

Manami Roychowdhury-Saha, Susan M. Lato, Eric D. Shank, and Donald H. Burke*

Department of Chemistry, Indiana University, Bloomington, Indiana 47405-7102

Received August 27, 2001; Revised Manuscript Received December 1, 2001

ABSTRACT: Flavin adenine dinucleotide (FAD) is one of the primary cofactors in biological redox reactions. Designing cofactor-dependent redox ribozymes could benefit from studies of new RNA−cofactor complexes, as would our understanding of ribozyme evolution during an RNA World. We have therefore used the SELEX method to identify RNA aptamers that recognize FAD. Functional analysis of mutant aptamers, S1 nuclease probing, and comparative sequence analysis identified a simple, 45 nt helical structure with several internal bulges as the core-binding element. These aptamers recognize with high specificity the isoalloxazine nucleus of FAD but do not distinguish FAD from $FADH_2$, nor are they removed from an FAD resin with UMP (which shares a pattern of hydrogen bond donors and acceptors along one face). Thus, these aptamers are structurally and functionally distinct from previously identified FMN and riboflavin aptamers. Circular dichroism data suggest a conformational change in the RNA upon FAD binding. These aptamers require magnesium and are active across a wide pH range (4.5−8.9). Since general acid−base catalysis plays a role in some flavin-dependent redox reaction mechanisms, these aptamers may be particularly well-suited to the design of new redox ribozymes.

Protein enzymes use several strategies to effect redox chemistry, such as using cysteine residues to donate or accept electrons temporarily. However, most redox enzymes rely on bound cofactors such as flavins, nicotinamides, and FeS centers, or combinations of these entities working together to effect electron transfer. Flavin adenine dinucleotide (FAD),[1] flavin mononucleotide (FMN), and several related compounds (Figure 1) are especially useful in that, unlike NAD^+, they can transfer either one or two electrons at a time. Many enzymes in central metabolism generate reduced flavins that are used in biosynthetic reductions or for shuttling reductive power into the electron transport chain. Flavoenzymes are found in glycolysis (pyruvate decarboxylase, the key link between glycolysis and the citric acid cycle), the citric acid cycle (such as α-ketoglutarate and succinate dehydrogenases), oxidative phosphorylation (3-phosphoglycerol oxidation by flavoprotein dehydrogenase), and fatty acid synthesis and oxidation. Glutathione reductase (which regulates the redox state of the glutathione pool, GSH:GSSG) is a flavoenzyme, as is mercuric reductase [which reduces toxic mercury salts and organomercuricials from Hg(II) to Hg(0)] (*1*). Flavins even serve as the chromophores for some proteins, such as photolyase (*2*) and various photoreceptors (chryptochrome and phototropins) (*3*−*5*). Their ubiquitous usage in so many facets of modern biochemistry suggests that nucleotide cofactors are likely to have been components of some of the first organisms to evolve.

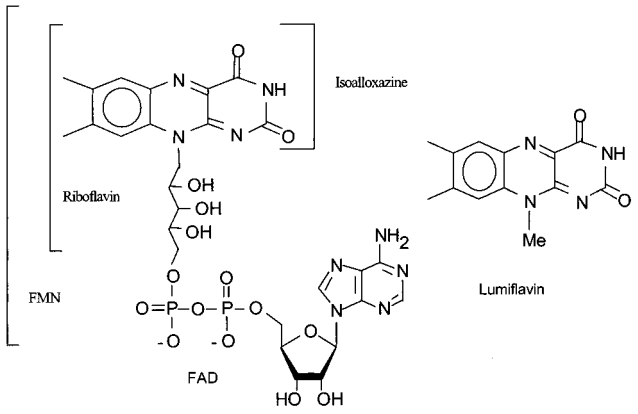

FIGURE 1: Structure of FAD and lumiflavin; riboflavin and FMN portions of FAD are marked.

Recent advances in the selection of new ribozymes (*6*−*11*) and in understanding the role of RNA catalysis within the ribosome (*12, 13*) have spurred enthusiasm for RNA World theories. These theories postulate an ancestral metabolism catalyzed by RNA molecules, though the complexity of that metabolism is debated. Adenosine cofactors (FAD, NAD^+, CoA, etc.) are sometimes viewed as molecular fossils left over from an RNA-based metabolic pathway (*14*−*16*). The chemically superfluous adenosine may have been covalently attached to the 5′ terminus (*17*) or within the chain (*16*) of RNA enzymes (ribozymes) that exploited dinucleotide cofactors to perform their respective reactions. Redox reactions have not yet been incorporated into the catalytic repertoire of in vitro-selected ribozymes, but two *deoxy*ribozymes with weak redox activity have been reported. Wilson

† This material is based upon work supported by the National Science Foundation under Grant 9896363.

* Correspondence should be addressed to this author. Phone: 812-856-4977. Fax: 812-855-8300. Email: dhburke@indiana.edu.

[1] Abbreviations: SELEX, Selective Evolution of Ligands by EXponential enrichment; FAD, flavin adenine dinucleotide, oxidized form; $FADH_2$, flavin adenine dinucleotide, reduced form; FMN, flavin mononucleotide; UMP, uridine monophosphate; GMP, guanosine monophosphate; ATP, adenosine triphosphate; dATP, deoxyadenosine triphosphate; NMN^+, nicotinamide mononucleotide, oxidized form; NAD^+, nicotinamide adenine dinucleotide, oxidized form; CoA, coenzyme A; GSSG, glutathione disulfide; GSH, glutathione; CD, circular dichroism.

10.1021/bi015719d CCC: $22.00
Published on Web 01/31/2002

and Szostak (*18*) found a sulforhodamine-binding DNA that promotes the oxidation of a structurally related fluorophore (dihydrotetramethylrosamine) in the presence of hydrogen peroxide (3.7-fold rate enhancement over uncatalyzed oxidation). Travascio et al. (*19*) described a hemin-binding 18-mer DNA molecule with peroxidase activity ($k_{cat}/K_M = 10^8$ M^{-1} s^{-1}) comparable to that of a catalytic antibody for the same reaction (*20*). Interestingly, both redox-active DNA catalysts form three-tiered G-quartet structures and bind their substrates with sub-micromolar affinities. However, RNA enzymes with redox activity and nucleotide cofactor-dependent RNA or DNA enzymes with redox activity have yet to be identified.

The design of cofactor-dependent redox ribozymes would be greatly facilitated by an expanded understanding of RNA−cofactor interactions. RNA aptamers to mononucleotide cofactors have led to significant progress in this area. FMN aptamers isolated by Burgstaller and Famulok assume a simple stem structure with an 11-nucleotide internal bulge (6 nucleotides on 1 strand, 5 on the other) (*21*, *22*). An NMR structure of this RNA showed that the isoalloxazine ring of FMN intercalates between a G·G mismatch and a G·U·A base-triple, and that the uracil-like edge of the isoalloxazine hydrogen-bonds to the Höogsteen edge of an adenine in the aptamer (*23*). Binding results from an induced fit mechanism, with the FMN contributing substantially to stabilization of the folded aptamer structure. Both the Breaker and Ellington groups have exploited this structural stabilization by incorporating the FMN-binding aptamer into the design of allosteric ribozymes whose self-cleavage (*24*) or self-ligation (*25*) reactions are stimulated nearly 300-fold in the presence of FMN because of structural stabilization upon binding the effector. Lauhon and Szostak have identified aptamers to mononucleoside redox cofactors (*26*). Their riboflavin aptamer appears to fold into a two-tiered G-quartet that binds both the oxidized and the reduced forms of the 5-deaza analogue of riboflavin. Since this RNA can be removed from a riboflavin resin with uracil, it presumably makes substantial contact with the base-pairing-like face of the isoalloxazine (*26*). Their aptamer to nicotinamide mononucleotide (NMN^+) appears to form a pair of helices separated by a three-nucleotide linker, and it shows approximately 15-fold discrimination between NMN^+ and its reduced form (*26*).

Since the dinucleotide cofactors appear to be of special evolutionary significance, it is worth having a better understanding of their interactions with RNA, both in biophysical terms and in terms of how the second nucleotide influences the SELEX process. Each of the aptamers to redox cofactors noted above also recognizes the flavin or nicotinamide portions of the corresponding dinucleotides, but there have also been selections targeted to bind the dinucleotides themselves. In these experiments, the adenosine portions of nucleotide cofactors have proven to be powerful SELEX targets. A pool selected to bind NAD^+ yielded an aptamer motif that recognized only the adenosine portion, ignoring the nicotinamide (*21*). Pools selected to recognize the pantotheine portion of CoA were similarly dominated by adenosine-binding aptamers, even though some of these selections included subtractive steps designed to exclude them from the pool (*27*, *28*). Another selection targeted against FAD yielded an aptamer that forms a generic helix capped with a 13-nucleotide, purine-rich loop (*21*). However, as we show below, this "FAD" aptamer recognizes the adenosine portion of the FAD molecule and is relatively nonspecific for purines in general.

We used SELEX to identify new FAD-binding RNA aptamers. Extensive analysis of the requirements for binding confirms that recognition is primarily through the isoalloxazine. The detail of the recognition specificity and the core RNA structure of the aptamers reported here are distinct from previously identified FAD-, riboflavin-, or FMN-binding RNAs. These new aptamers reveal the evolutionary potential for cofactor binding by RNA aptamers, expand the catalog of RNAs targeted to nucleotide cofactors, and may aid in the design and construction of nucleotide-dependent redox ribozymes.

EXPERIMENTAL PROCEDURES

Materials. DNA oligos were synthesized by Integrated DNA Technologies (Coralville, IA), radionucleotides were obtained from ICN, and all chemicals and affinity resins are from Sigma (St. Louis, MO).

Nucleic Acid Manipulations. In vitro transcription with phage T7 RNA polymerase was performed using the Ampliscribe kit (Epicenter, Madison, WI) under standard conditions. Gel-purified RNA was dissolved in water and the concentration determined by measuring the absorbance at 260 nm. After every round of selection, recovered RNAs were reverse-transcribed using Superscript II RT (Gibco BRL, Grand Island, NY) and amplified using Taq DNA polymerase, following standard procedures. Limited digestion with S1 nuclease (Promega) used 0.5 unit of the enzyme with 50 μM $ZnCl_2$ at room temperature. T1 nuclease ladders were generated with 0.1 unit of enzyme (Epicenter, Madison, WI) for 10 min at 50 °C. For partial alkaline hydrolysis, RNA was heated to 90 °C for 8 min in carbonate buffer, pH 9.5, then neutralized and ethanol-precipitated for boundary determinations, or directly frozen in dry ice for use as a size ladder. 5′ end-labeling was performed using [γ-^{32}P]ATP and T4 polynucleotide kinase. 3′ labeling was done by annealing an oligonucleotide which was complementary to the 3′ end of the RNA with a TTT overhang. Klenow extension with [α-^{32}P]dATP gave 3′ radiolabeled RNA (*29*).

Selections and Analogue Assays. Radiolabeled RNA was unfolded in water at 70 °C and allowed to refold at room temperature in 1× binding buffer (50 mM Bis-Tris, pH 6.4, 200 mM NaCl, and 10 mM $MgCl_2$). Folded RNA was preincubated with FAD resin (immobilized through ribose hydroxyls) and filtered through a 1 cm^3 syringe containing glass wool to arrest the resin. After removing nonbinding RNAs by washing with 10 column volumes of binding buffer, specifically bound species were eluted with 6 column volumes of 5 mM FAD solution in 1× binding buffer. The amount of RNA in each fraction was measured using Cherenkov counting.

Boundary Determination. Partially hydrolyzed RNA fragments were partitioned on the FAD affinity resin without preincubation. Wash and elution fractions were pooled separately and then run on an 8% denaturing sequencing gel. FAD was removed from the elution fractions using Amicon-10 microconcentrator spin filters (Amicon, Beverly, MA) before loading on the gel to prevent FAD-dependent anomalous migration. The boundaries were assigned by comparison to a T1 nuclease digestion ladder.

FIGURE 2: Some sequences from the selection of FAD-binding aptamers from the 80N pool. The entire 80N region has not been shown; lower case nucleotides represent the primer region, and those underlined represent the consensus region. Black wedges show the 3′ functional boundaries; numbers in parentheses represent the multiple times that individuals have been isolated. The PCR product of the FAD-binding region (shown by the arrow) was made using appropriate primers to test their binding affinity; the dotted arrow represent sequences whose entire 5′ primer region has not been shown. A list of all the sequences is available at http://ernie.chem.indiana.edu/~dhburke/all_seqs.html.

K_d Studies. For spin filtration measurements, RNA was equilibrated with [^{3}H]riboflavin (ICN) (0.1 μM) at room temperature for 10 min and spun through an Amicon-10 microconcentrator at 13 000 rpm for 4 min. The difference in ^{3}H counts in 25 μL fractions from each side of the membrane as determined by Cherenkov counting was taken as an indication of riboflavin accumulation above the membrane, and served as the basis for calculating K_d as described (*27*). For isocratic elution studies (*30*), RNA was loaded onto the FAD resin and washed with 55 column volumes of buffer that contained various concentrations of FAD, and then any remaining RNA was eluted with 5 mM FAD. Median elution volumes were taken as the point at which half of the total had been eluted. The reported K_d values reflect the average and standard deviations for two independent sets of measurements, each using five different FAD concentrations plus a buffer-only sample.

Circular Dichroism. The CD spectrum was measured in the wavelength range of 200−300 nm at 0.5 nm intervals and a speed of 10 nm/min. Cuvettes of 1 mm path length were used. The signal sensitivity was 200 mdeg, and the slit width was set at 3000 μm. CD spectra were recorded using various combinations of RNA, FAD, and FMN in the binding buffer.

RESULTS

Selection, Sequences, Activity Screen. FAD-binding RNA aptamers were isolated using the SELEX method on an FAD affinity matrix. The starting pool, which has been used previously to identify aptamers to HIV-1 RT (*31*), *S*-adenosylmethionine (*32*), and coenzyme A (*27*), contained approximately 10^{14} different species. The 54 sequences obtained from the eighth round pool all included variations on the consensus 5′-CAAGAAAGATGTC-3′ (most highly conserved nucleotides underlined), located at various positions throughout the 80 nucleotide random region (Figure 2). This motif is not present in any of the aptamers previously selected to recognize flavin- or adenosine-containing cofactors.

Boundaries, Deletions, and Structural Models. Three approaches were used to determine the secondary structures of these FAD aptamers. First, deletion−selection experiments established the 5′ and 3′ functional boundaries for four isolates: F8.18, F8.35, F8.59, and F8.62. End-labeled RNA was partially alkaline-hydrolyzed, and then allowed to bind the FAD affinity resin. Samples from the load, wash, and elution fractions were analyzed using denaturing gel electrophoresis by comparing them to the input hydrolysis ladder and to a partial T1 nuclease digestion ladder (which cleaves 3′ to guanosines). The smallest fragment recovered during specific elution of 5′ end-labeled RNA from the resin defines the 3′-most nucleotide required for binding activity. In each case, the 3′ functional boundary is within two nucleotides of the 3′ end of the consensus motif. Synthetic oligonucleotide primers were used to amplify transcription templates that included sequences from the original 5′ primer-binding region through the identified consensus for 4 isolates [F8.35, which yields an 82 nucleotide RNA, F8.12 (45 nt), F8.27 (45 nt), and F8.64 (64 nt)] (arrows in Figure 2). In each case, the shortened RNA was retained on the column and specifically eluted at least as efficiently as the full-length aptamers (134 nt), confirming the 3′ functional boundaries. Using 3′ end-labeled RNA, there was no evidence that any bases could be removed from the 5′ end to within the resolution of the gel (1−3 nucleotides). The locations of functional boundaries are expected to be in positions where deletion of a small number of bases would disrupt the functional structure. Sequences near the 5′ ends of these RNAs can form a four base pair helix with the 3′ end of the conserved motif. Shortening this helix by one or two base pairs is expected to destabilize it, consistent with the functional boundary data. Figure 3a shows one structure that includes this helix.

In the second approach, 37 mutant RNAs were generated to compare the effects of nucleotide changes at various positions. Strengthening stem 1 by appending three new base pairs (Ftest10, Figure 3b) or by changing the A5-U42 pair to C-G increased the elution signal, confirming that stem 1 does indeed form. Data for stem 2 were more ambiguous. Changing the U-A pair in the middle of stem 2 to a C-G or G-C pair was expected to strengthen this stem. Instead, about a third as much of the mutant carrying the C-G could bind and elute from the FAD resin as compared to RNAs carrying the original U-A pair, while changing it to a G-C or A-U pair abolished binding activity altogether. These data must be interpreted cautiously, however, since all of these stem 2 variants are predicted by Mfold (*33*) to form different structures compared to Ftest1, so they may not represent conservative substitutions. We conclude that stem 2 is either

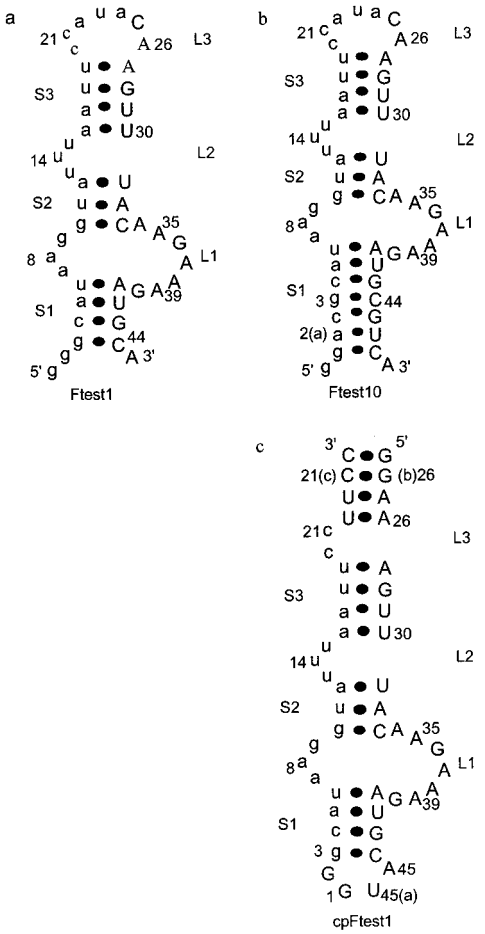

FIGURE 3: Secondary structures of (a) Ftest1, (b) Ftest10, and (c) cpFtest1. Lowercase letters represent primer-binding regions from the original selection for FAD. Numbering in all the structures is based on that of Ftest1 for ease of comparison; letters after the number indicate 3′ insertion, and letters before the number indicate 5′ insertion, not present in wt.

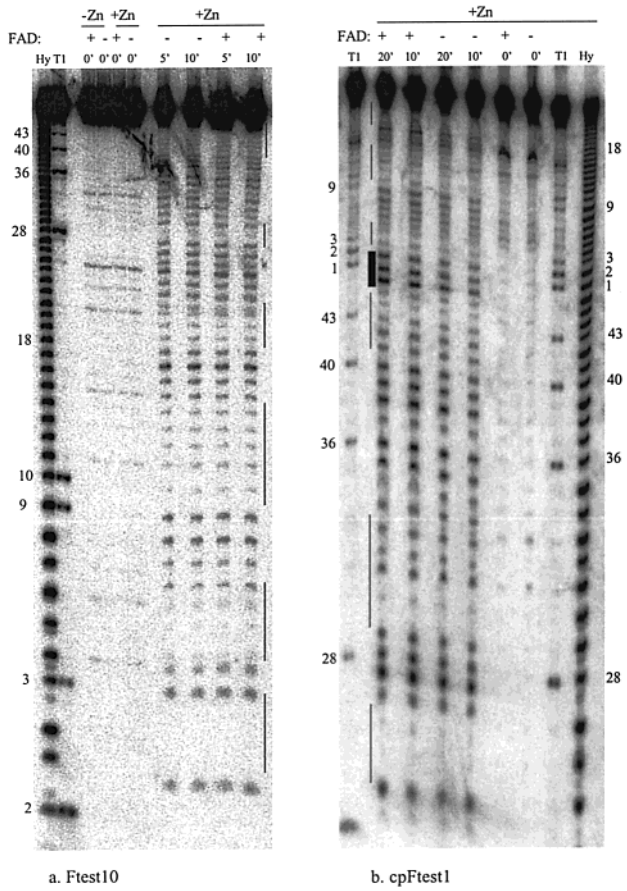

FIGURE 4: S1 nuclease protection patterns of (a) Ftest10 and (b) cpFtest1. FAD was used at 500 μM for Ftest10 and 1 mM for cpFtest1 where indicated with (+). Vertical lines indicate the base-paired region, the black rectangle indicates enhanced sensitivity to S1 nuclease in the presence of FAD, and the numbering of the bands is based on the secondary structure shown in Figure 3.

required to be of a particular sequence [it may contact the FAD directly (see below) or serve to position the U3 loop relative to loops 1 and 2] or that it may not form at all. To test the importance of stem 3, a circularly permuted mutant was generated in which transcription was initiated at C25 (two G's were appended to allow use of the T7 promoter) and ended at A24, and the 4 bp stem 1 was closed with an AUGG tetraloop (Figure 3c). Retention of the mutant on the column was about one-third wild-type. Extending the relatively weak, permuted stem 3 with four additional base pairs restored activity. Retention values for additional mutants show that there is no specific sequence requirement for stem 3 (not shown). Shortening loop 3 from seven nucleotides (CCAUACA) to three (CCA) or replacing it with an unrelated tetraloop (GAGA) increased the elution signal 1.5-fold. Combined with the results from the circular permutations and the lack of constraints at these positions among the originally selected sequences, these data demonstrate that stem 3 does indeed form, and that the loop at the end of stem 3 has no direct role in binding FAD. The smaller terminal loops in the mutants appear to stabilize stem 3 against the breathing that is suggested in the S1 digestion pattern (below). Cytosine scanning mutagenesis, in which one nucleotide at a time was changed to C, was used to probe the roles of nucleotides at internal bulge positions (U13, U14, U15, and A35 through G40). For all nine RNAs, the substitution to C abolished FAD binding. An alternative structural model pairs nucleotides U13−U15 with a subset of the purines in the large conserved loop; however, none of the mutations designed to test such pairings was active (e.g., U14G/U15G/A38C/A39C) (see Supporting Information for a detailed list of all mutants).

Finally, end-labeled RNA was challenged with S1 nuclease, which preferentially cleaves unstructured RNA. The S1 nuclease cleavage pattern supports a structure with several paired regions. Both strands of stem 1 in Ftest1 (positions 3−6 and 41−44) are less susceptible to enzymatic cleavage relative to the loop positions. This protection is especially evident in an "extended-stem" RNA oligo (Ftest10, 50mer) (compare vertically within individual lanes in Figure 4a), which shows a higher percentage of RNA retained on the FAD resin as compared to the parent molecule (Ftest1, 45mer). There is similar protection in the stem 2 region and partial protection in the stem 3 region. Residual sensitivity in stem 3 may arise from breathing of the molecule. Further support for this secondary structure comes from the S1 digestion pattern of cpFtest1, a circular permutation of Ftest1 (49mer, Figures 3c and 4b), which shows more efficient retention on the FAD resin than that observed for Ftest1. The closing loop of cpFtest1 (nucleotides 45a, 1, 2) shows

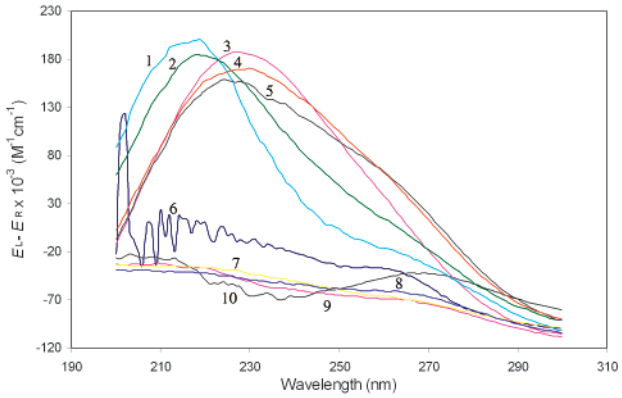

FIGURE 5: CD spectrum of Ftest1 RNA with different concentrations of FAD or FMN. The numbered traces are (1) cyan = 15 μM RNA + 500 μM FAD, (2) green = 15 μM RNA + 250 μM FAD, (3) pink = 15 μM RNA only, (4) orange = 15 μM RNA + 250 μM FMN, (5) dark green = 15 μM RNA + 500 μM FMN, (6) navy blue = 1× binding buffer alone, (7) yellow = 250 μM FMN in buffer, (8) blue = 500 μM FMN in buffer, (9) purple = 250 μM FAD, and (10) black = 500 μM FAD.

enhanced cleavage upon FAD binding, which may arise due to a conformational change of the aptamer that make this loop more accessible for enzymatic cleavage. Interestingly, the postulated U3 bulge is protected from cleavage by S1 in both the absence and the presence of FAD, and it may be inherently structured. All of the data above are consistent with an FAD-binding structure similar to the one shown in Figure 3, which includes three internal loops and a central stem—all of which are highly constrained—and two flanking stems that are more tolerant of substitutions.

Ligand-Binding Analysis. Isocratic elution (*30*) from the FAD resin in various concentrations of FAD gave a dissociation constant, K_d, of 50 ± 20 μM (data not shown). This estimate is consistent with spin filtration measurements (*34*), which gave a lower limit of 5 μM. The circular dichroism spectrum of aptamer Ftest1 is characteristic of A-form RNA, and the wavelength of maximal ellipticity is blue-shifted in the presence of FAD (Figure 5). The shift is concentration-dependent as evidenced from the spectral signatures at 250 and 500 μM FAD. The isosbestic point in the spectrum is suggestive of a "two-state" conformational change upon complex formation. Although the net retention efficiencies of both FAD and FMN are similar, there is no blue shift in the spectrum of the FMN−RNA complex (Figure 5). Differences in the CD spectra of the two complexes may reflect some difference in their modes of binding. For example, although the AMP portion is not required for the binding interaction (see below), it may participate in formation of the complex in an isoenergetic manner, contributing to its CD spectral character but not noticeably to the overall affinity.

Binding Conditions. The conditions under which a selection is carried out can have profound effects on the outcome of that selection. For example, CoA aptamers selected under slightly acidic conditions were later shown to be inactive at neutral or alkaline pH (*27*), and trace metals included in ribozyme selections are found in several cases to be required for their catalytic activities (*7*, *35*−*37*). The FAD selection in this study was carried out in a buffer containing 10 mM $MgCl_2$, 200 mM NaCl, and 50 mM Bis-Tris, pH 6.4. To

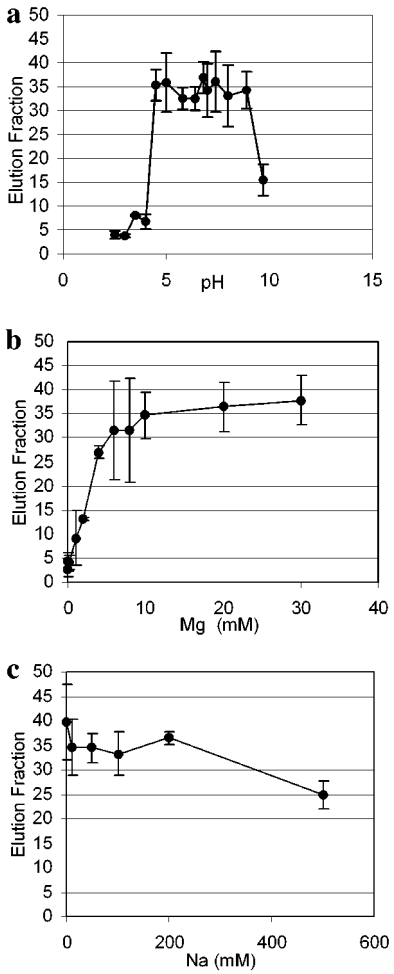

FIGURE 6: Binding efficiencies as a function of (a) pH, (b) Na^+ concentration, and (c) Mg^{2+} concentration; averages of three data points were plotted.

test the importance of each of these components, the 82 nucleotide truncated form of aptamer F8.35, F8.35.82, was folded in normal binding buffer, applied to FAD resin that had been equilibrated with various candidate buffers, washed with the same candidate buffer, and eluted with FAD in the same buffer. The fraction of the applied RNA that was retained under these conditions was taken as an indication of how well the alternate buffer supported folding of the aptamer (Figure 6). Binding to the FAD resin tolerated a surprisingly wide range of pH's, with no significant difference in binding efficiency from pH 4.5 (acetate buffer) to pH 8.9 (AMPSO buffer). Binding dropped off sharply at pH 9.5 and above or at pH 4.0 and below, probably due to titration of the bases. Magnesium is required for binding, with half-maximal elution observed between 2 and 4 mM, and little improvement as concentrations were increased beyond 10 mM. No significant binding was observed below 1 mM Mg^{2+}. In the presence of sodium concentrations of 0−200 mM, RNA bound and eluted with equivalent efficiency, with some reduction at 500 mM.

Target Specificity. The specificity of molecular recognition can be determined readily through competitive elution with various analogues of FAD (Table 1 and Figure 1). Radiolabeled RNA from isolate F8.35.82 was bound to the FAD resin, washed with buffer, eluted with 500 μM analogue, and then stripped with 5 mM FAD. Of the total RNA

Table 1: Analogue Assays on F8.35.82[a]

0.5 mM FAD	74%	0.5 mM TTP	30%
0.5 mM FMN	66 ± 8%	saturated lumichrome	20%
saturated riboflavin	73%	0.5 mM AMP	16%
0.5 mM TMP	14 ± 4%	theophyline	20%
5 mM TMP	23%	caffeine	27%
saturated lumiflavin	63 ± 11%	xanthosine	26%

[a] 100% corresponds to the sum of (RNA eluted by analogue) + (RNA subsequently eluted by 5 mM FAD).

removed from the column, the percentage removed during the analogue phase is an indication of how completely that analogue satisfied the requirements for recognition (*27*). When FAD was itself used as the "analogue" under these conditions, 77% of the eluted RNA was removed during the analogue phase. Analogues containing the adenine base but missing the isoalloxazine (adenine, adenosine, AMP, ATP) were unable to elute the bound RNA, whereas compounds that contained the isoalloxazine ring eluted the RNA with approximately the same efficiency as FAD itself (FMN, riboflavin). Replacing the N5 ribose of riboflavin with a single methyl group ("lumiflavin") or with a proton ("lumichrome") gave elutions with intermediate efficiency; however, these compounds are not sufficiently soluble to allow direct comparison. Therefore, the isoalloxazine ring, or some portion of it, is necessary for recognition, and little if any of the ribose is needed. To rule out the possibility that the lack of elution by the analogues is due to kinetic limitations, the aptamer was preincubated 5 min with 100 μM AMP or GMP prior to incubating 5 min with FAD resin (equilibrated with 100 μM analogue). The prior presence of the analogue and its inclusion during the wash fractions had no effect on the amount of RNA retained on the FAD resin relative to inverting the order of addition (data not shown, available as Supporting Information), ruling out the possibility that kinetic considerations might have prevented our observing interactions with AMP or GMP.

Several additional analogues were tested to evaluate the contributions of various components of the isoalloxazine ring itself. First, nucleotides whose Watson−Crick faces mimic the uracil-like side of isoalloxazine (TMP, TTP, IMP, xanthosine, hypoxanthine, xanthine, and GMP) were unable to elute the bound RNA. Mixtures of these analogues were also ineffective (TMP + AMP, TMP + adenosine). We cannot rule out the possibility that the uracil-like face of the flavin plays some role in recognition, but it is clearly not as significant as in the case of the FMN−aptamer complex, in which an adenosine base in the aptamer makes an A-U-like pair with the flavin (*21*). Interestingly, caffeine and theophylline, whose methylated rings are more hydrophobic than the purines alone, gave intermediate elution efficiencies. To evaluate the importance of the redox state of the flavin, FAD on the resin was reduced to $FADH_2$ in an anaerobic chamber before RNA was added. The RNA bound the reduced resin and was eluted efficiently with $FADH_2$, demonstrating that this aptamer recognizes both redox states, and that it probably does not make essential hydrogen bonds with the two redox-active nitrogens.

Similar specificity assays were applied to a stem−loop RNA that had been previously identified in a selection for FAD aptamers (27FAD-1) (*21*) (Figure 7). As expected, FAD eluted 27FAD-1 RNA from the FAD resin, consistent with

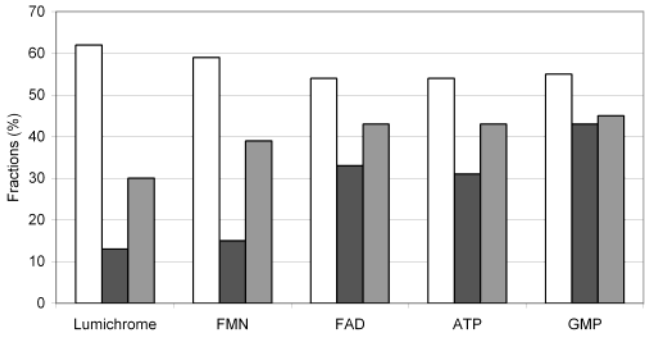

FIGURE 7: Analogue assays with the previously identified "FAD" aptamer, 27-FAD-1: 5′ GGCAGUCGAAAGG AAGUGUAGA-CUGCC 3′ (*21*). The concentration of FAD, FMN, ATP, and GMP used for elution was 1 mM; a saturated solution of lumichrome was used, due to its lower solubility. The final elution (strip) was carried out with 5 mM FAD solution to establish the total amount of RNA that was available to be eluted; white bars, total RNA removed during washes; black bars, RNA eluted by analogues; gray bars, sum of analogue elutions plus strips (see Experimental Procedures).

previous observations. However, ATP alone gave a similar elution percentage, and GMP eluted still more RNA. Furthermore, both lumiflavin and FMN, which lack the adenosine portion of FAD, eluted less RNA than FAD, ATP, or GMP. The stem−loop aptamer should thus be considered to recognize purines in a relatively nonspecific manner, rather than specifically as an FAD aptamer. The aptamers selected in the present work are therefore the first to have been both targeted to FAD and to bind specifically the portion of the cofactor involved in the redox chemistry.

DISCUSSION

Prospects for Redox Ribozymes. The ease with which small molecule−RNA complexes are recovered from random pools is often taken as an important indication that not all catalytic reactions in the RNA World need have been carried out by the RNA alone; bound cofactors such as FAD may have been used in redox and other reactions. The aptamers identified in this study may be especially useful in the design of modern flavin-dependent redox ribozymes. They bind to both the reduced and the oxidized forms of the flavins, allowing selection of catalysts for either reduction or oxidation reactions. Their tolerance of a wide range of pH conditions (4.5−8.9) can be exploited to promote general acid−base catalysis, which is often a feature of flavin reactivity. For example, the N1 of $FADH_2$ is often deprotonated during flavin-dependent two-electron reduction reactions, causing increased electron density to accumulate within the ring system that facilitates hydride transfer from N5. The reverse reaction, hydride transfer to FAD (flavin-dependent oxidation reactions), requires a protonation step to neutralize the negative charge.

The lack of binding specificity between FAD and $FADH_2$ suggests that the redox-active hydrides may not be deeply buried. It is therefore possible that the binding site, or a minor modification of that binding site, may accommodate a potential redox substrate to effect one- or two-electron transfer. Other ways in which flavin-dependent redox reactions can be favored—such as precise positioning of cofactors, charge stabilization in transition states and intermediates, and

activation of nucleophiles and electrophiles—are established activities for ribozymes. Identification of ribozymes that use nucleotide cofactors to effect oxidation−reduction reactions may be more a function of choosing an appropriate selection system than of limitations in the underlying chemistry.

Evolution of Aptamers to Nucleotide Cofactors. There are now three independent aptamers known to bind flavins. The "FMN aptamer" (*21*) is the best known of these and the one on which the most extensive structural and functional information is available. The G-quartet aptamer selected to bind riboflavin (*26*) also binds a variety of other flavin cofactors, but like the "FMN aptamer" was selected in the context of only one aromatic system. This work describes a small, simple RNA element that binds both the oxidized and the reduced forms of FAD, and is the only one that was selected in the context of intact FAD.

The present selection for aptamers to FAD did not yield any aptamer that interacted solely with the adenosine portion; the isoalloxazine nucleus was the recognition core, with high elution fractions obtained for FMN, riboflavin, and lumiflavin and no significant elution observed for AMP or ribose 5-phosphate. This is in contrast to RNA pools selected to recognize other adenosine cofactors, such as NAD^+ (*21*), SAM (*32*), CoA (*27, 28*), and even another selection targeted to FAD (*21*). Each of these produced adenosine-binding RNAs to the exclusion of molecules that uniquely recognized other portions of the respective targets. The only element of our selection that does not find an equivalent in previous efforts to target FAD is the arbitrary choice of a different primer-binding sequence, and these sequences are involved in forming the active structure (lower case in Figure 3). There was no aspect of our selection specifically designed to exclude adenosine recognition, though such specificity could easily have been enforced through counterselection steps; for example, RNAs that recognize AMP could have been removed by including AMP in the wash steps.

Adenosine's effectiveness as a target for eliciting RNA aptamers has implications for the evolution and engineering of cofactor-dependent RNA catalysis. Ribozymes involved in acyltransfers, phosphorylations, methyl transfers, and redox reactions could each be designed with a common adenosine-binding module at the core of their respective cofactor-binding elements. Similarly, during RNA World evolution, once such a core was established for one of these classes of enzymes, variations could proliferate for use in other ribozymes, similar to the proliferation of the Rossman fold for nucleotide cofactor binding by protein enzymes. On the other hand, enzymes for each of these reactions could benefit from contacts that orient or activate the reactive portions of the respective cofactors. The present work shows that it is not inevitable for selections to adenosine cofactors to be dominated by aptamers to the adenosine portion, and that more direct evolutionary pathways are also available.

ACKNOWLEDGMENT

We thank Andrew Paulsel, Tia Milanese, Rebecca Schein, and Lori Scates for technical assistance, Gary Stormo and Laurie Heuyer for help with early sequence analysis, and Larry Gold for providing laboratory space and resources during the early stages of this work.

SUPPORTING INFORMATION AVAILABLE

A list of RNA sequences used in the mutagenesis study and their relative retention values on the FAD resin has been provided as supporting information. Data for the competitive binding assays comparing order of addition are also provided. This material is available free of charge via the Internet at http://pubs.acs.org.

REFERENCES

1. Misra, T. (1992) *Plasmid 27*, 4−16.
2. Jorns, M., Sancar, G., and Sancar, A. (1984) *Biochemistry 23*, 2673−2679.
3. Christie, J. M., Reymond, P., Powell, G. K., Bernasconi, P., Raibekas, A. A., Liscum, E., and Briggs, W. R. (1998) *Science 282*, 1698−1701.
4. Salomon, M., Christie, J. M., Knieb, E., Lempert, U., and Briggs, W. R. (2000) *Biochemistry 39*, 9401−9410.
5. Lin, C., Robertson, D. E., Ahmad, M., Raibekas, A. A., Jorns, M. S., Dutton, P. L., and Cashmore, A. R. (1995) *Science 269*, 968−970.
6. Illangasekare, M., and Yarus, M. (1999) *RNA 5*, 1482−1489.
7. Illangasekare, M., Sanchez, G., Nickels, T., and Yarus, M. (1995) *Science 267*, 643−647.
8. Lee, N., Bessho, Y., We, I. K., Szostak, J., and Suga, H. (2000) *Nat. Struct. Biol. 7*, 28−33.
9. Unrau, P. J., and Bartel, D. P. (1998) *Nature 395*, 260−263.
10. Seelig, B., Keiper, S., Stuhlmann, F., and Jaschke, A. (2000) *Angew. Chem., Int. Ed. Engl. 15*, 4576−4579.
11. Johnston, W., Unrau, P., Lawrence, M., Glasner, M., and Bartel, D. (2001) *Science 292*, 1319−1325.
12. Nissen, P., Hansen, J., Ban, N., Moore, P., and Steitz, T. (2000) *Science 289*, 920−930.
13. Muth, G., Ortoleva-Donnelly, L., and Strobel, S. (2000) *Science 289*, 947−950.
14. Benner, S. A., Ellington, A. D., and Tauer, A. (1989) *Proc. Natl. Acad. Sci. U.S.A. 86*, 7054−7058.
15. Benner, S. A., Cohen, M. A., Gonnet, G. H., Berkowitz, D. B., and Johnsson, K. P. (1993) in *The RNA World* (Gesteland, R. F., and Atkins, J. F., Eds.) pp 27−70, CSHL Press, Plainview, NY.
16. White, H., III (1976) *J. Mol. Evol. 7*, 101−104.
17. Huang, F., Bugg, C., and Yarus, M. (2000) *Biochemistry 39*, 15548−15555.
18. Wilson, C., and Szostak, J. W. (1998) *Chem. Biol. 5*, 609−617.
19. Travascio, P., Bennet, A. J., Wang, D. Y., and Sen, D. (1999) *Chem. Biol. 6*, 779−787.
20. Cochran, A. G., and Schultz, P. G. (1990) *J. Am. Chem. Soc. 112*, 9414−9415.
21. Burgstaller, P., and Famulok, M. (1994) *Angew. Chem., Int. Ed. Engl. 33*, 1084−1087.
22. Burgstaller, P., and Famulok, M. (1996) *Bioorg. Med. Chem. Lett. 6*, 1157−1162.
23. Fan, P., Suri, A. K., Fiala, R., Live, D., and Patel, D. J. (1996) *J. Mol. Biol. 258*, 480−500.
24. Soukup, G., and Breaker, R. (1999) *Proc. Natl. Acad. Sci. U.S.A. 96*, 3584−3589.
25. Robertson, M., and Ellington, A. (2000) *Nucleic Acids Res. 28*, 1751−1759.
26. Lauhon, C. T., and Szostak, J. W. (1995) *J. Am. Chem. Soc. 117*, 1246−1257.
27. Burke, D. H., and Hoffman, D. C. (1998) *Biochemistry 37*, 4653−4663.
28. Burke, D. H., Saran, D., Frank, J., and Malhi, A. (2002) (in preparation).

29. Huang, Z., and Szostak, J. W. (1996) *Nucleic Acids Res. 24*, 4360−4361.
30. Connell, G. J., Illangasekare, M., and Yarus, M. (1993) *Biochemistry 32*, 5497−5502.
31. Burke, D. H., Scates, L. A., Andrews, K., and Gold, L. (1996) *J. Mol. Biol. 264*, 650−666.
32. Burke, D. H., and Gold, L. (1997) *Nucleic Acids Res. 25*, 2020−2024.
33. Mathews, D., Sabina, J., Zuker, M., and Turner, D. (1999) *J. Mol. Biol. 288*, 911−940.
34. Jenison, R. D., Gill, S. C., Pardi, A., and Polisky, B. (1994) *Science 263*, 1425−1429.
35. Tasarow, T. M., Tasarow, S. L., and Eaton, B. E. (1997) *Nature 389*, 54−57.
36. Wiegand, T. W., Janssen, R. C., and Eaton, B. E. (1997) *Chem. Biol. 4*, 675−683.
37. Huang, F., and Yarus, M. (1997) *Biochemistry 36*, 14107−14119.

BI015719D